FEEDBACK DESCENT: OPEN-ENDED TEXT OPTIMIZATION VIA PAIRWISE COMPARISON

Anonymous authors
Paper under double-blind review

ABSTRACT

Current preference learning methods discard the rich explanations humans naturally provide when comparing examples, collapsing detailed feedback into binary signals. We introduce *Feedback Descent*, a framework that widens this information bottleneck by leveraging textual feedback to enable directed optimization in text space rather than weight space. We show that in-context learning can transform structured feedback into gradient-like directional information, enabling targeted edits of text artifacts such as prompts, code, and JSON. Unlike prior approaches that collapse judgments into single bits, our evaluators pair each comparison with textual feedback, which functions as high-bandwidth supervision. The iteration loop is done purely at inference time, without modifying any model weights, and is task-agnostic. We evaluate Feedback Descent on three diverse domains and find that it outperforms state-of-the-art prompt optimization (GEPA), reinforcement learning methods (GRPO, REINVENT), and even specialized graph-based molecular optimizers. In the DOCKSTRING molecule discovery benchmark, Feedback Descent identifies novel drug-like molecules surpassing the 99.9th percentile of a database with more than 200,000 compounds across six protein targets.

1 INTRODUCTION

A central goal of machine learning is building systems that can perform tasks that are difficult or impossible even for humans. Reinforcement learning is a powerful framework that accomplishes this goal, since it can optimize with respect to feedback on its own outputs, rather than relying on supervised examples of desired outputs. Indeed, recent language models have demonstrated impressive feats in domains like math and programming (OpenAI, 2024; DeepSeek-AI et al., 2025; Google DeepMind, 2025; Zhu et al., 2024) through a combination of reinforcement learning and text-based reasoning. Unfortunately, existing reinforcement learning frameworks are designed to learn from impoverished supervision signals, typically either scalar rewards or pairwise preference data, where each annotation conveys at most a single bit per pair. These bottlenecks discard information about *why* one behavior is better and *how* to improve—information available in environment feedback or easily elicited from humans during annotation.

Our goal is to widen this information bottleneck, i.e., significantly increase the information the system can extract per unit of experience (Silver & Sutton, 2025). Collecting more detailed feedback is straightforward, e.g., with brief rationales explaining preferences; the challenge is turning such feedback into measurable improvement. Because free-form feedback does not define a differentiable objective, it cannot directly drive weight updates via backpropagation. Our core idea is to use an *optimization loop in text space* rather than weight space: we leverage the in-context learning capabilities of language models to translate feedback into targeted edits of text artifacts (e.g., code, prompts, molecules, JSON configs, etc) that improve a final performance objective.

To that end, we introduce *Feedback Descent*, a framework for continual optimization in text space. At each iteration, we generate a new candidate artifact based on all previous feedback. We compare this candidate against the current best artifact, and the evaluator returns a preference along with textual feedback explaining the choice. If the candidate is preferred, it becomes the new best. Repeating this loop yields semantically local, feedback-aligned improvements that implement gradient-like steps in text space. See Fig. 1 for a conceptual illustration. We provide theoretical intuition for why Feedback Descent can be effective. Under appropriate assumptions about feedback quality

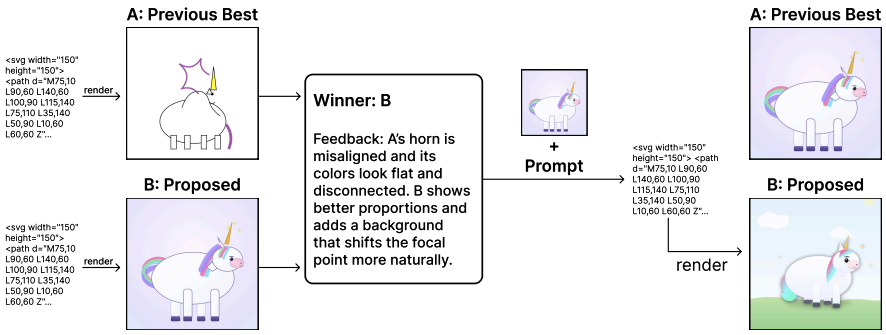

Figure 1: A conceptual illustration of feedback descent. At each iteration, we compare the previous best artifact with a new candidate. The evaluator provides both a pairwise preference and textual feedback. Preferences ensure the selection of better candidates, while feedback accumulates directional information that guides semantically meaningful edits.

and problem structure, we demonstrate that textual feedback can provide directional information, enabling efficient optimization.

Our contributions are threefold. First, we introduce *Feedback Descent*, an inference-time optimization framework that uses pairwise preferences with textual rationales to provide directional updates entirely in text space. Second, we demonstrate its generality across three domains: (i) SVG design, where iterative feedback produces judge-aligned visual improvements beyond direct prompting under both scratch and rubric-aware initializations; (ii) prompt optimization on IFBench, where Feedback Descent surpasses GEPA on Qwen3-8B and remains competitive with the strongest methods on GPT-4.1 Mini; and (iii) molecule discovery on DOCKSTRING, where Feedback Descent outperforms reinforcement learning approaches such as REINVENT and rivals specialized graph-based algorithms. Third, we show that the novel molecules discovered by Feedback Descent exceed not only the 99.9th percentile of a 260,000-compound database but, on several targets, surpass the best molecule present in the dataset.

2 Feedback Descent: Open-Ended Text Optimization

We propose Feedback Descent, a framework for open-ended optimization of text-native artifacts whose quality is easier to *judge* than to *construct*. Feedback Descent converts comparative textual feedback into directed semantic edits and iterates in a self-improvement loop. As a running example, consider optimizing SVG code to render better images of a unicorn. Current vision-language models can reliably compare two renderings and explain the choice, even if writing high-quality SVG from scratch is difficult. Through Feedback Descent, we can convert these explanations into directed edits that aim to produce an artifact that is better than all previous ones.

2.1 Problem Setup

Let $\mathcal{S}$ be the space of token sequences, and let $x \in \mathcal{S}$ denote an artifact (e.g., SVG code). Given a current incumbent $x_t^\star \in \mathcal{S}$ and a candidate $x \in \mathcal{S}$, the evaluator returns

$$\mathsf{E}(x, x_t^\star) \to \big(p \in \{0,1\},\ r \in \mathcal{S}\big), \tag{1}$$

where $p = 1$ indicates $x \succ x_t^\star$ and r is a textual feedback explaining *why* the winner is better and *how* to improve. We append r_t to a history $\mathcal{R}_t = \{(x_1, r_1), \ldots, (x_t, r_t)\}$ and iterate, keeping track of the current best artifact $x_t^\star$.

2.2 Feedback Descent

Feedback Descent operates as an iterative optimization loop that maintains a single best artifact x_t^* and progressively improves it through feedback-guided mutations and comparative evaluation. Throughout, we use $\mathcal{M}$ to denote the language model used for generating improved candidates.

Initialization and termination. We initialize x_0^* by prompting a language model with the task description alone (e.g., "Generate SVG code for a unicorn"), providing a reasonable starting point

without prior feedback. The algorithm runs for a fixed budget of T iterations or until convergence (defined as no improvement for k consecutive iterations).

Proposing semantic mutations via prompting. The mutation step leverages a language model's in-context learning capabilities. Given the current best artifact x_t^* and accumulated feedback $r_1, r_2, \ldots, r_{t-1}$, we prompt the model to generate improved candidates:

$$x_t = \mathcal{M}\left(\text{“Improve } x_t^* \text{ using feedback: } \mathcal{R}_{t-1}\text{”}\right) \tag{2}$$

These prompts are intentionally minimal: the optimization signal comes from the accumulated feedback rather than heavy prompt engineering. They include basic task context, the current best artifact, and feedback from previous comparisons. Complete prompt templates for each domain are provided in Appendix C.3.

Algorithm 1 Feedback Descent

Require: Initial text x_0, Language model $\mathcal{M}$, T

```
Current best: x* ← x_0, Rationale history: R ← ∅
for t = 1 to T do
    x_t ← M(x*, R)                          ▷ Propose (2)
    p_t, r_t ← COMPARE(x_t, x*)             ▷ Compare (1)
    R ← R ∪ {(x_t, r_t)}
    if p_t = 1 then
        x* ← x_t, R ← ∅                     ▷ Update + reset
return x*
```

Selection and update. We compare the new candidate x_t against the current best x_t^* using the evaluator $\mathsf{E}(x_t, x_t^*)$, which returns both a binary preference p_t and a textual feedback r_t. In our running SVG example, examples of feedback include “adjust the stroke width”, “make sure the legs are connected to the body”, and “add a shadow to the unicorn's mane”. Regardless of the preference outcome, we always add the feedback to our history: $\mathcal{R}_{t+1} = \mathcal{R}_t \cup \{(x_t, r_t)\}$. If $p_t = 1$ (candidate is preferred), we update $x_{t+1}^* = x_t$; otherwise we keep $x_{t+1}^* = x_t^*$. We summarize the overall process in Algorithm 1.

2.3 Analogy to Gradient Descent

The key algorithmic insight is best understood by analogy to the gradient descent algorithm. Just as gradients provide the direction of steepest ascent under local linearity, textual feedback can suggest plausible directions of improvement in semantic space. For our SVG example, if the feedback indicates “needs more defined horn shape,” we expect that a small edit to the horn shape that preserves overall structure will likely be an improvement.

Of course, textual feedback is not a literal gradient. It is approximate and occasionally contradictory—optimization with such feedback does not have convergence guarantees in the same way that gradient descent does. Instead, feedback acts as a heuristic directional cue, offering higher-bandwidth supervision than a binary preference signal or a scalar reward, just as first-order optimization is fundamentally faster than zeroth-order optimization (Nemirovski & Yudin, 1983; Agarwal et al., 2012; Nesterov & Spokoiny, 2017). We hypothesize that an open-ended optimization loop based on such cues can succeed, supported by prior evidence that language models reliably translate textual instructions into concrete modifications. Examples include generating code changes (Chen et al., 2021; Austin et al., 2021; Nijkamp et al., 2022; Wang et al., 2023b; Roziere et al., 2023; Guo et al., 2024; Lozhkov et al., 2024; CodeGemma Team et al., 2024), following complex multi-step instructions (Ouyang et al., 2022; Wei et al., 2022a; Chung et al., 2022; Longpre et al., 2023; Zhang et al., 2024), targeted text modifications (Schick et al., 2022; Du et al., 2022; Madaan et al., 2023; Welleck et al., 2023; Kim et al., 2023), and decomposing high-level goals into executable action sequences (Schick et al., 2023; Parisi et al., 2022; Yao et al., 2023b; Qin et al., 2023; Wang et al., 2023a; Agarwal et al., 2025).

We emphasize that this gradient analogy serves only as an intuition: gradients indicate directions in continuous parameter space, while rationales indicate directions in semantic space, without guarantees of smoothness or convergence. Our experiments in Section 5 demonstrate that feedback-guided optimization indeed produces consistent improvements across tasks, validating that such heuristic directional cues are sufficient to drive open-ended text optimization.

3 Directional Information is Critical When Effective Dimensionality is High

In this section, we give intuition for why and when Feedback Descent is particularly effective, using a minimal idealized model of directional information based on comparisons with feedback. We provide simplified statements here, and show full proofs in Appendix A.

Pairwise preference alone is a binary signal: it tells us which artifact is better but not *how* to improve. Adding a short rationale (*"legs disconnected from body; increase stroke width"*) turns each comparison into a *directional cue* in semantic space. Iterating this loop accumulates such cues, allowing a mutator LLM to make small, targeted edits that are more likely than chance to increase quality. Even when individual rationales are imperfect, the *aggregate* message across failures (what kept losing and why) continually refines the direction of improvement.

As an idealized model, map each text x to a latent feature $z = \phi(x) \in \mathbb{R}^d$ with utility $r(z) = R(x)$, where d denotes the effective dimensionality of the semantic space. Let $z^\star = \arg\max_z r(z)$ be the optimum. For problems of interest, d may be in the hundreds or thousands, reflecting the many degrees of freedom in text, molecule, or image design spaces.

A rationale r_t is *useful* if its induced edit defines a direction v_t positively correlated with the gradient $\nabla r(z_t)$. Under this model, feedback carries gradient information and systematically reduces error, yielding linear convergence in expectation, even with imperfect rationales.

Proposition 1 (Directional updates achieve dimension-free convergence, informal)**.** *Suppose we perform N rationale-guided updates, where each update direction v_t is on average positively aligned with $\nabla r(z_t)$. Then the expected error after N evaluations satisfies*

$$\mathbb{E}[\, r(z^\star) - r(z_N)\,] \;\le\; (1-\alpha)^N\, [r(z^\star) - r(z_0)],$$

for some constant $\alpha > 0$ depending only on the alignment and variability of the feedback. Crucially, this rate does not depend on the dimension d.

While rationale-guided updates exploit directional information to achieve convergence rates that do not depend on the ambient dimension, methods that rely only on function evaluations or binary preferences suffer severe dimension-dependent slowdowns:

Proposition 2 (Inefficiency of zeroth-order search, informal)**.** *Consider zeroth-order methods with N evaluations in $\mathbb{R}^d$. For a strongly concave quadratic, to reach ϵ-accuracy one needs at least*

$$N \;\ge\; (c/\epsilon)^{d/2},$$

and best-of-N random sampling achieves at best

$$\mathbb{E}[\, r(z^\star) - r(z_N)\,] = \Omega(N^{-2/d}).$$

Thus, while rationale-guided updates drive $r(z_N)$ toward $r(z^\star)$ at a dimension-free linear rate, zeroth-order search suffers exponential slowdowns as d grows.

We emphasize that these propositions are highly idealized, serving only to illustrate a general principle: in high-dimensional search, even weak directional cues can accumulate into steady improvement, whereas unguided search scales exponentially worse. Thinking in terms of a continuous latent space is a pragmatic abstraction; modern ML operates on continuous weights and embeddings that approximate local structure even in discrete domains. By the same logic, many forms of human progress, including writing, coding, and science, often arise from successive refinements within implicit semantic space shared by experts. The following statements are for motivational clarity, **not** literal models of the systems in Section 5.

The propositions rest on well-known results in optimization and combinatorics. Our contribution is applying this intuition to open-ended text optimization, where it highlights effective dimensionality as the key bottleneck. To our best knowledge, the closest prior work that adopts this framing is the empirical taxonomy and optimizer design of Nie et al. (2024); building on their study, we identify effective dimensionality as the key limiting factor, showing that in open-ended settings where artifacts admit many possible alterations, even weak but aligned textual rationales provide the directional information needed for linear convergence, while zeroth-order methods degrade exponentially.

Implications. First, even imperfect cues accelerate optimization when aggregated, since their consistent positive correlation with the gradient accumulates into reliable directional information. Second, in problems with high effective dimensionality, where exploration can proceed in unbounded directions, pure zeroth-order search becomes extremely inefficient. In this regime, obtaining directed feedback on the most salient aspects, whether from experimental results, an expert's feedback, or exploiting a generator-verifier gap, is essential for sustained progress. This is especially important for open-ended problems where the optimum is not known in advance.

Directional Information is Advantageous in High Dimensions

Unlike zeroth-order methods, which scale poorly with dimension, Feedback Descent remains effective when the effective dimensionality is high because feedback provides directional cues that guide optimization.

4 Related Work

Preference Learning. Preference learning methods learn from pairwise comparisons (Christiano et al., 2017; Ouyang et al., 2022; Azar et al., 2023; Ethayarajh et al., 2024; Munos et al., 2024); recent advances include bypassing the need for a reward model (Rafailov et al., 2023), iterative optimization under KL constraints (Xiong et al., 2023), and adaptive scaling techniques (Wang et al., 2024). However, these methods fundamentally compress complex human reasoning into binary or scalar preferences, foregoing the rich explanatory content that humans can naturally provide alongside judgments (Wirth et al., 2017). Unlike prior work that relies solely on scalar feedback despite the complexity of human judgment, we leverage detailed textual rationales to widen this information bottleneck, allowing for more efficient adaptation.

Gradient-Free Optimization. Zeroth-order optimization methods (Chen et al., 2019) operate without access to gradients, typically achieving convergence rates that scale poorly with dimension. While the black-box nature of modern LLMs has spurred interest in applying gradient-free approaches (Guo et al., 2023; Sun et al., 2022; Chen et al., 2024; Lange et al., 2024), these methods face fundamental challenges in high-dimensional spaces. Our approach explores whether textual rationales can provide useful directional information for optimization, similar to how Nie et al. (2024) shows that LLMs can be effective optimizers when provided with directional feedback from historical traces.

Optimizing Compound AI Systems. Compound AI systems, i.e., modular architectures involving multiple LLM invocations and complex control flow, such as agents or scaffolding techniques (Yao et al., 2023b), present unique optimization challenges due to their modularity. Several approaches have emerged to tackle this complexity, including optimization for searching and bootstrapping few-shot in-context examples (Khattab et al., 2022; 2024; Opsahl-Ong et al., 2024), backpropagating textual feedback between components (Yuksekgonul et al., 2024), and reflective prompt evolution (Agrawal et al., 2025). However, these methods focus on optimizing individual components or connections within fixed architectures. In contrast, Feedback Descent provides a general-purpose text optimization framework that treats LLMs as optimizers for any text-representable artifact. While compound AI systems are one promising application domain, our approach generalizes beyond AI systems to optimize standalone text artifacts such as SVG code and molecular representations.

Inference-Time Optimization for LLMs. Inference-time optimization improves performance without weight updates by performing additional computation at generation. This paradigm includes self-critique and refinement cycles (constitution-guided critique (Bai et al., 2022); Self-Refine (Madaan et al., 2023)) test-time scaling via best-of-N, multi-step reasoning, and tree search (Cobbe et al., 2021; Zelikman et al., 2022; Yao et al., 2023a), and iterative prompt optimization (Zhou et al., 2022; Yang et al., 2023; Pryzant et al., 2023). Several works report that strategically allocating inference-time compute yields large gains (Snell et al., 2024; Brown et al., 2025; Geiping et al., 2025; Zhou et al., 2025). We build on the growing consensus that natural language is a particularly powerful medium for inference-time improvement. Natural language traces enable models to reason effectively in complex environments (Lampinen et al., 2022; Wei et al., 2022b), and language models can reliably map textual instructions to concrete modifications (Chen et al., 2021; Austin et al., 2021; Saunders et al., 2022; Scheurer et al., 2023). However, existing methods often rely on random sampling of self-generated critiques, which may be noisy or fail to capture external preferences. In contrast, we leverage external rationales as directional information, enabling guided search in the semantic space.

Model	Condition	Anatomy	Cyber	Geom	Min.	Retro	Story	Avg
GPT-4o-mini	Scratch	100.0	100.0	93.8	100.0	100.0	100.0	99.0
	Informed	100.0	85.7	84.6	84.6	15.4*	92.9	77.2
GPT-5-mini	Scratch	100.0	100.0	100.0	100.0	100.0	100.0	100.0
	Informed	100.0	81.8	94.4	93.8	94.1	100.0	94.0

Table 1: Win rates after five iterations comparing Feedback Descent against direct prompting under two conditions: from *Scratch* and *Informed* of the judge rubric. Values above 50% indicate that Feedback Descent outperforms the baseline; *denotes the only failure case where direct prompting wins. **Iterative feedback consistently improves SVG designs over direct prompting.**

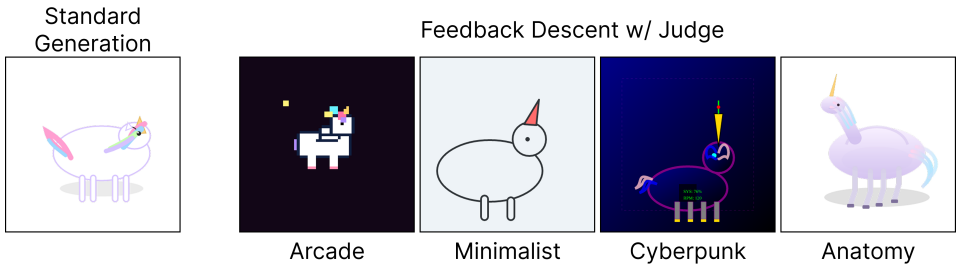

Figure 2: Example unicorn images generated by Feedback Descent under four different judge criteria: retro arcade, minimalist, cyberpunk, and anatomy. **Feedback Descent yields visually distinct unicorns aligned with the aesthetic criteria preferred by each judge.**

5 Experiments

We evaluate Feedback Descent across three diverse domains—visual design, prompt optimization, and molecule discovery—to demonstrate its generality and effectiveness. Through our experiments, we aim to answer the following questions. First, we ask whether Feedback Descent exhibits generality by working robustly across qualitatively different domains. Second, we test sample efficiency, evaluating whether iterative, rationale-guided feedback enables higher-quality solutions with fewer model queries than existing optimizers. Third, we measure outcome quality, assessing whether Feedback Descent can produce artifacts (SVGs, prompts, and molecules) that not only satisfy rubrics and constraints but also surpass state-of-the-art methods on established benchmarks.

5.1 Experimental Domains

We describe each evaluation domain and how we obtain pairwise comparisons augmented with textual rationales.

SVG optimization. Taking inspiration from Bubeck et al. (2023), we ask models to output SVG code for illustrations of unicorns. We use a set of six diverse judge prompts, each preferring a different aesthetic: accurate *anatomy*, *cyberpunk* futurism, *geometric* abstraction, *minimalist*, *retro arcade* pixel-art motifs, and *storybook* illustrations. We compare rendered SVGs using `GPT-5-mini`, which outputs both a binary preference and short textual feedback. To mitigate order bias, we perform two judgments with swapped image orders (A-B and B-A) and declare a winner only if both judgments are consistent. Otherwise, we try again, up to three times, and discard if no consistent winner emerges.

Prompt optimization. We follow the setup of GEPA (Agrawal et al., 2025) on IFBench (Pyatkin et al., 2025), a benchmark for evaluating precise constraint-following (e.g., "answer only with yes or no"). We design a two-stage system that first produces an answer and then rewrites it to satisfy constraints, and we jointly optimize the prompts for both stages using Feedback Descent. Optimization is driven by the 150 training examples: candidate prompts are updated based on performance on the training set and textual feedback describing which constraints were satisfied or violated. All candidate prompts are scored on the 300 validation examples, and the prompt with the highest validation accuracy rate is selected. We report performance on a test set of 294 held-out examples.

Method	Qwen3-8B	GPT-4.1 Mini
DSPy Default (Khattab et al., 2024)	36.90	47.79
MIPROv2 (Opsahl-Ong et al., 2024)	36.22	49.15
GRPO (Shao et al., 2024)	35.88	—
GEPA (Agrawal et al., 2025)	38.61	52.72
GEPA+Merge (Agrawal et al., 2025)	28.23	**55.95**
Ours	**44.22**	54.59

Table 2: Comparison of prompt optimization methods on IFBench. We report scores for Qwen3-8B and GPT-4.1 Mini under matched rollout budgets. **Feedback Descent outperforms all baselines on Qwen3-8B, and is competitive with the state-of-the-art for GPT-4.1 Mini.**

Molecule discovery. We evaluate on molecular docking tasks using DOCKSTRING (García-Ortegón et al., 2022) docking scores and drug-likeness (QED). DOCKSTRING provides a realistic drug discovery setting where molecules are evaluated based on their predicted binding affinity to medically relevant targets rather than simple physicochemical properties. We focus on challenging optimization tasks across six protein targets: ADRB1, PGR, PPARA, PPARG, CDK2, and F2. Following DOCKSTRING, we compute the combined score $s = -\text{Vina} - 10 \times (1 - \text{QED})$. We represent molecules as SMILES strings (Weininger, 1988) and evaluate using DOCKSTRING's molecular docking pipeline to compute Vina scores (binding affinity). The feedback system provides rich structured information, including RDKit molecular descriptors (Landrum, 2006), similarity searches against known compounds from molecular databases (Liu et al., 2007; Gilson et al., 2016; Gaulton et al., 2012; Mendez et al., 2019), and detailed docking results. In the system prompt, we also provide the LLM information about the protein target obtained from the UniProt database (The UniProt Consortium, 2023). Together, this provides the LLM with detailed feedback on molecular properties that affect binding affinity, drug-likeness violations, and comparisons to known active compounds.

5.2 SVG Optimization

We evaluate iterative feedback against direct prompting across two generators, `GPT-4o-mini` and `GPT-5-mini`. The direct prompting baseline receives the full evaluation rubric and is tasked with producing a single best design. Feedback Descent instead begins with an initial set of candidates, and through 5 rounds of structured feedback and improvement, refines designs using judge comparisons that reflect aesthetic criteria. We test two initialization regimes: **Scratch**, which starts from images simply instructed to generate images of unicorns, and **Informed**, which starts from the strongest direct generations conditioned on the rubric, determined by the LLM judge.

Results. Table 1 shows the win rates after 5 iterations. For both `GPT-4o-mini` and `GPT-5-mini`, Feedback Descent reliably improves outputs over the initial population. Furthermore, qualitative examples in Fig. 2 demonstrate that the procedure consistently produces unicorns whose visual style diverges across judges, aligning with aesthetic criteria such as geometry, minimalism, or retro arcade motifs.

Iterative feedback can elicit better outputs from the same model

Because of a generator–verifier gap, even prompting with the exact judge rubric is suboptimal for SVG generation. Feedback Descent elicits better images from the same generator by iteratively proposing improvements guided by feedback.

5.3 Prompt Optimization

We compare Feedback Descent against five baselines: the default prompt implemented in the DSPy program (Khattab et al., 2024, Default), a Bayesian optimization approach for selecting instructions and demonstrations (Opsahl-Ong et al., 2024, MIPROv2), online reinforcement learning (Shao et al., 2024, GRPO), and a reflective prompt evolution method (Agrawal et al., 2025, GEPA). All baselines are run under matched rollout budgets for fair comparison, and the reported baseline results are from Agrawal et al. (2025).

	Method	ADRB1	PGR	PPARA	PPARG	CDK2	F2
DOCKSTRING (N=260155)	50% Percentile	5.305	3.478	4.549	4.210	4.385	4.168
	90% Percentile	8.785	7.878	7.987	7.658	7.733	7.477
	99% Percentile	9.620	8.703	8.718	8.449	8.453	8.139
	99.9% Percentile	10.209	9.260	9.230	9.012	8.979	8.722
	99.99% Percentile	10.742	9.723	9.821	9.518	9.509	9.252
	Best	11.330	9.742	9.907	9.529	9.534	9.311
	SMILES GA (Brown et al., 2019)	9.358	8.313	8.785	8.423	7.773	7.642
	REINVENT (Olivecrona et al., 2017)	9.971	8.711	9.083	9.179	8.314	8.284
	GP-BO† (Tripp et al., 2021)	10.284	9.332	9.709	9.404	8.987	8.125
	Graph MCTS† (Jensen, 2019)	7.464	7.179	7.555	7.520	6.481	5.326
	Graph GA† (Jensen, 2019)	9.883	9.364	**10.200**	8.931	8.577	8.023
	Feedback Descent (Ours)	**10.623**	**9.615**	9.919	**10.187**	**9.803**	**9.300**

Table 3: Comparison of molecule optimization methods on six protein targets. Fragment-based algorithms (denoted by †) operate directly on molecular graphs, giving them structural priors unavailable to purely text-based methods. For each target, the top generative result is in **bold**, and any population in the DOCKSTRING dataset that exceeds the best generative result is underlined. **Feedback Descent rivals or surpasses specialized molecular optimizers across all six targets.**

Each example produces pointwise feedback about which constraints were satisfied or violated. To construct the pairwise feedback for Feedback Descent, we stratify the examples into quadrants based on whether each prompt resulted in a correct response. We then ask the model to propose textual descriptions of inputs where these discrepancies arise. We then statistically validate each hypothesis, filtering for ones that correspond to consistent differences in performance between the prompts. This process distills the true global differences between the two prompts.

Table 2 shows that Feedback Descent achieves the highest score on Qwen3-8B (44.22 vs. 38.61 for GEPA) and remains competitive with GEPA and GEPA+Merge on GPT-4.1 Mini (54.59 vs. 55.95). These results indicate that structured, iterative feedback drives steady improvements in prompt optimization, even though other optimizers such as GEPA exploit problem structure.

Grounded Summaries Enable Reliable Prompt Optimization

By summarizing a large set of pointwise rationales into a global comparison between two prompts, Feedback Descent yields more reliable prompts.

5.4 Molecule Optimization (DOCKSTRING)

We compare against baselines implemented in the `mol_opt` repository (Gao et al., 2022), Our comparisons include a genetic algorithm (Brown et al., 2019, SMILES GA), reinforcement learning (Olivecrona et al., 2017, REINVENT), fragment-based algorithms (Jensen, 2019, Graph MCTS/GA), and Bayesian optimization on molecular graphs (Tripp et al., 2021, GP-BO). Because fragment-based methods exploit graph-level structural priors, the most direct comparison is to the text-only baselines: SMILES-GA and REINVENT. Nonetheless, we report results against all methods to provide a complete picture of performance. **Results.** Table 3 summarizes optimization outcomes across six protein targets. For each target, we benchmark Feedback Descent against specialized molecular optimization algorithms as well as ligands from the DOCKSTRING dataset, which comprises both decoy and experimentally active ligands. Feedback Descent is competitive with all baselines and achieves the strongest scores on several targets (e.g., ADRB1, PGR, PPARG, CDK2, F2). On multiple proteins, it matches or exceeds the 99.9th and even 99.99th percentiles of the DOCKSTRING database, including surpassing the best molecule present in the dataset itself ($N = 260155$). These findings show that Feedback Descent, a purely text-based method, can rival or outperform

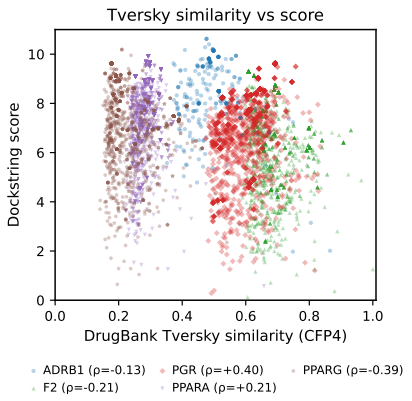

Figure 3: Scatter plots of Tversky similarity to approved drugs against docking scores, showing weak or negative correlations across targets. **High-scoring molecules discovered by Feedback Descent are far from any known drugs.**

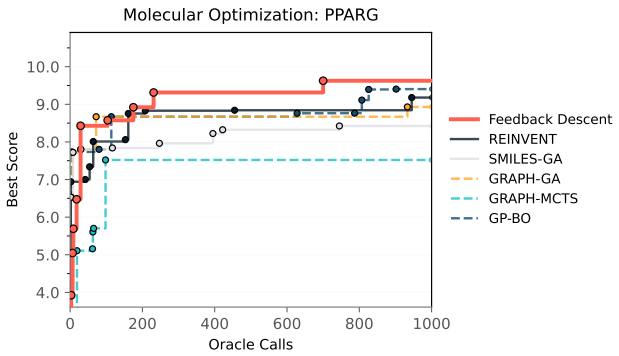

Figure 4: Optimization trajectories on PPARG showing docking scores over oracle calls for Feedback Descent and specialized baselines. **Feedback Descent quickly improves molecular docking scores within the first few hundred oracle calls.**

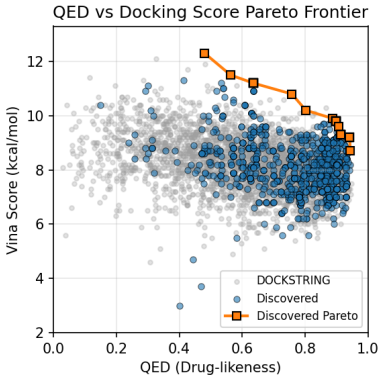

Figure 5: Pareto frontier of docking affinity vs. drug-likeness, comparing Feedback Descent molecules (blue) to the DOCKSTRING dataset (gray). **Feedback Descent finds novel molecules that meet or surpass known ones.**

specialized graph-based algorithms, despite lacking handcrafted structural priors. Fig. 4 shows optimization trajectories for PPARG. Feedback Descent achieves competitive trajectories relative to specialized methods, often reaching high-scoring regions of chemical space with comparable or fewer oracle calls. This pattern holds across targets, suggesting that the method generalizes rather than relying on idiosyncrasies of a single protein system.

Analysis of discovered molecules. Fig. 5 illustrates the Pareto frontier between docking affinity (Vina score) and drug-likeness (QED) for PPARG. Feedback Descent recovers molecules that sit on or above the DOCKSTRING frontier, indicating that improvements in affinity are not achieved at the expense of reduced drug-likeness. See Fig. 6 in the appendix for the full set of Pareto frontiers across all targets. These results show that feedback-guided search yields candidates that are not only potent but also balanced along multiple drug-relevant dimensions.

We also examine novelty by plotting Tversky similarity (CFP4 fingerprints) to approved DrugBank molecules against docking scores in Fig. 3. Across all targets, the correlations are weak or negative (Spearman ρ between -0.39 and 0.40), showing that high-scoring candidates discovered by Feedback Descent do not simply recycle functional groups from existing drugs but instead explore novel regions of chemical space. For CDK2, no comparison is shown: the target lacks any fully approved drugs in DrugBank with orthosteric binding as part of their mechanism of action, and thus does not satisfy our filtering criteria for inclusion.

Feedback Descent Can Discover Novel Targeted Molecules

Feedback Descent, operating in a purely textual form, consistently identifies novel molecules that surpass high-percentile baselines in DOCKSTRING. This demonstrates that iterative, feedback-guided optimization can enable models to genuinely explore unknown design spaces beyond their training distribution.

6 Discussion

This paper presents Feedback Descent, an inference-time framework that improves text artifacts through structured pairwise feedback. We validate it on visual design, prompt optimization, and molecule discovery, showing that text can serve as an optimizable medium, not just static data. Unlike parameter tuning, this approach can leverage richer textual signals, allowing for continual improvement without requiring retraining.

Limitations. The method relies on strong evaluators, which may be scarce in some domains. Training models to produce reliable feedback remains a prerequisite for harder tasks. For creative domains, strictly "following the gradient" may be limiting; balancing refinement with exploration is an important next step.

Ethics Statement

This work adheres to the ICLR Code of Ethics. Our research focuses on improving preference learning methods through textual rationales, which have positive implications for AI alignment and human-AI collaboration. The methods developed could potentially be misused to optimize for harmful content; the same risk exists with any preference learning approach. Our contribution lies in making such optimization more efficient rather than enabling fundamentally new capabilities.

Reproducibility Statement

We are committed to ensuring the reproducibility of our results. Complete experimental details, including hyperparameters and evaluation protocols, are provided in the main text and appendix. All datasets used in our experiments are either publicly available or will be released upon publication. The proofs are presented with full detail in Appendix A with all assumptions clearly stated. Implementation details for Feedback Descent, including prompting strategies and in-context learning procedures, are documented in the appendix.

References

Alekh Agarwal, Peter L Bartlett, Pradeep Ravikumar, and Martin J Wainwright. Information-theoretic lower bounds on the oracle complexity of stochastic convex optimization. *IEEE Transactions on Information Theory*, 58(5):3235–3249, 2012.

Mayank Agarwal, Ibrahim Abdelaziz, Kinjal Basu, Merve Unuvar, Luis A Lastras, Yara Rizk, and Pavan Kapanipathi. Toolrm: Outcome reward models for tool-calling large language models. *arXiv preprint arXiv:2509.11963*, 2025.

Lakshya A Agrawal, Shangyin Tan, Dilara Soylu, Noah Ziems, Rishi Khare, Krista Opsahl-Ong, Arnav Singhvi, Herumb Shandilya, Michael J Ryan, Meng Jiang, et al. Gepa: Reflective prompt evolution can outperform reinforcement learning. *arXiv preprint arXiv:2507.19457*, 2025.

Jacob Austin, Augustus Odena, Maxwell I. Nye, Maarten Bosma, Henryk Michalewski, David Dohan, Ellen Jiang, Carrie J. Cai, Michael Terry, Quoc V. Le, and Charles Sutton. Program synthesis with large language models. *arXiv preprint arXiv:2108.07732*, 2021.

Mohammad Gheshlaghi Azar, Mark Rowland, Bilal Piot, Daniel Guo, Daniele Calandriello, Michal Valko, and Remi Munos. A general theoretical paradigm to understand learning from human preferences. *arXiv preprint arXiv:2310.12036*, 2023.

Yuntao Bai, Saurav Kadavath, Sandipan Kundu, Amanda Askell, Jackson Kernion, Andy Jones, Anna Chen, Anna Goldie, Azalia Mirhoseini, Cameron McKinnon, et al. Constitutional ai: Harmlessness from ai feedback. *arXiv preprint arXiv:2212.08073*, 2022.

Nathan Brown, Marco Fiscato, Marwin HS Segler, and Alain C Vaucher. Guacamol: Benchmarking models for de novo molecular design. *Journal of Chemical Information and Modeling*, 59(3): 1096–1108, 2019. doi: 10.1021/acs.jcim.8b00839.

Tom B. Brown et al. s1: Simple test-time scaling. *arXiv preprint arXiv:2501.19393*, 2025.

Sébastien Bubeck, Varun Chandrasekaran, Ronen Eldan, Johannes Gehrke, Eric Horvitz, Ece Kamar, Peter Lee, Yin Tat Lee, Yuanzhi Li, Scott Lundberg, et al. Sparks of artificial general intelligence: Early experiments with gpt-4. *arXiv preprint arXiv:2303.12712*, 2023.

Mark Chen, Jerry Tworek, Heewoo Jun, Qiming Yuan, Henrique Ponde de Oliveira Pinto, Jared Kaplan, Harri Edwards, Yura Burda, Nicholas Joseph, Greg Brockman, Alex Ray, Raul Puigdomenech, Alec Radford, Vedant Sastry, Ilya Sutskever, Daniel M. Ziegler, Amanda Dennison, Marius Ervin, William Perez, Sallaheddine Karaa, Sarah Kluska, Jerome Lespiau, Tom B. Brown, and David Wu. Evaluating large language models trained on code. *arXiv preprint arXiv:2107.03374*, 2021.

Xiangyi Chen, Sijia Liu, Kaidi Xu, Xingguo Li, Xue Lin, Mingyi Hong, and David Cox. Zo-adamm: Zeroth-order adaptive momentum method for black-box optimization. 2019.

Xiangyi Chen, Sijia Liu, and Mingyi Hong. Derivative-free optimization for low-rank adaptation in large language models. *arXiv preprint arXiv:2403.01754*, 2024.

Paul F Christiano, Jan Leike, Tom Brown, Miljan Martic, Shane Legg, and Dario Amodei. Deep reinforcement learning from human preferences. *Advances in Neural Information Processing Systems*, 30, 2017.

Hyung Won Chung, Le Hou, Shayne Longpre, Barret Zoph, Yi Tay, William Fedus, Eric Li, Xuezhe Wang, Mostafa Dehghani, Siddhartha Brahma, Albert Webson, Shixiang Shane Gu, Zhuyun Dai, Mirac Suzgun, Xinyun Chen, Aakanksha Chowdhery, Sharan Narang, Gaurav Mishra, Adams Yu, Vincent Zhao, Yanping Huang, Andrew Dai, Hongkun Yu, Slav Petrov, Ed H. Chi, Jeff Dean, Jacob Devlin, Adam Roberts, Denny Zhou, Quoc V. Le, and Jason Wei. Scaling instruction-finetuned language models. *arXiv preprint arXiv:2210.11416*, 2022.

Karl Cobbe, Vineet Kosaraju, Mohammad Bavarian, Mark Chen, Heewoo Jun, Lukasz Kaiser, Matthias Plappert, Jerry Tworek, Jacob Hilton, Reiichiro Nakano, Christopher Hesse, and John Schulman. Training verifiers to solve math word problems. *arXiv preprint arXiv:2110.14168*, 2021.

CodeGemma Team, Heri Zhao, et al. Codegemma: Open code models based on gemma. *arXiv preprint arXiv:2406.11409*, 2024.

DeepSeek-AI, Daya Guo, Dejian Yang, Haowei Zhang, Junxiao Song, Ruoyu Zhang, Runxin Xu, Qihao Zhu, Shirong Ma, Peiyi Wang, et al. Deepseek-r1: Incentivizing reasoning capability in llms via reinforcement learning. *arXiv preprint arXiv:2501.12948*, 2025. URL https://arxiv.org/abs/2501.12948.

Wanyu Du, Vipul Raheja, Dhruv Kumar, Zae Myung Kim, Melissa Lopez, and Dongyeop Kang. Read, revise, repeat: A system demonstration for human-in-the-loop iterative text revision. *In2Writing*, 2022.

Kawin Ethayarajh, Winnie Xu, Niklas Muennighoff, Dan Jurafsky, and Douwe Kiela. Kto: Model alignment as prospect theoretic optimization. *arXiv preprint arXiv:2402.01306*, 2024.

Wenhao Gao, Tianfan Fu, Jimeng Sun, and Connor W Coley. Sample efficiency matters: A benchmark for practical molecular optimization. *arXiv preprint arXiv:2206.12411*, 2022.

Miguel García-Ortegón, Gregor N. C. Simm, Austin J. Tripp, José Miguel Hernández-Lobato, Matthias R. Bauer, and Sergio Bacallado. Dockstring: Easy molecular docking yields better benchmarks for ligand design. *Journal of Chemical Information and Modeling*, 62(15):3486–3502, 2022. doi: 10.1021/acs.jcim.1c01334.

Anna Gaulton, Louisa J Bellis, A Patricia Bento, Jon Chambers, Mark Davies, Anne Hersey, Yvonne Light, Shaun McGlinchey, David Michalovich, Bissan Al-Lazikani, and John P Overington. Chembl: a large-scale bioactivity database for drug discovery. *Nucleic Acids Research*, 40(D1): D1100–D1107, 2012. doi: 10.1093/nar/gkr777.

Jonas Geiping, Sean McLeish, Neel Jain, John Kirchenbauer, Siddharth Singh, Brian R Bartoldson, Bhavya Kailkhura, Abhinav Bhatele, and Tom Goldstein. Scaling up test-time compute with latent reasoning: A recurrent depth approach. *arXiv preprint arXiv:2502.05171*, 2025.

Michael K Gilson, Tiqing Liu, Michael Baitaluk, George Nicola, Linda Hwang, and Justin Chong. Bindingdb in 2015: a public database for medicinal chemistry, computational chemistry and systems pharmacology. *Nucleic Acids Research*, 44(D1):D1045–D1053, 2016. doi: 10.1093/nar/gkv1072.

Google DeepMind. Gold-medalist performance in solving olympiad geometry with alphageometry2. *arXiv preprint arXiv:2502.03544*, 2025. URL https://arxiv.org/abs/2502.03544.

Daya Guo, Shuo Ren, Shuai Lu, Zhangyin Feng, Duyu Tang, Shijie Liu, Long Zhou, Nan Duan, Alexey Svyatkovskiy, Shengyu Fu, et al. Deepseek-coder: When the large language model meets programming – the rise of code intelligence. *arXiv preprint arXiv:2401.14196*, 2024.

Zerui Guo, Tianxiang Sun, Xipeng Qiu, and Xuanjing Huang. When gradient descent meets derivative-free optimization: A match made in black-box scenario. *arXiv preprint arXiv:2305.10013*, 2023.

Jan H Jensen. A graph-based genetic algorithm and generative model/monte carlo tree search for the exploration of chemical space. *Chemical Science*, 10(12):3567–3572, 2019. doi: 10.1039/C8SC05372C.

Omar Khattab, Christopher Potts, and Matei Zaharia. Demonstrate-search-predict: Composing retrieval and language models for knowledge-intensive nlp. *arXiv preprint arXiv:2212.14024*, 2022.

Omar Khattab, Arnav Singhvi, Paridhi Maheshwari, Zhiyuan Zhang, Keshav Santhanam, Sri Vardhamanan, Saiful Haq, Ashutosh Sharma, Thomas T Joshi, Hanna Moazam, Heather Miller, Matei Zaharia, and Christopher Potts. Dspy: Compiling declarative language model calls into self-improving pipelines. *arXiv preprint arXiv:2310.03714*, 2024.

Seonghyeon Kim, Sukmin Cho, Doyoung Kim, Sejin Kim, Chacha Chen, Ekaterina Kochmar, Hwajung Hong, and Alice Oh. Help me think: A simple prompting strategy for non-experts to create customized content with models. *arXiv preprint arXiv:2208.08232*, 2023.

Andrew K Lampinen, Nicholas Roy, Ishita Dasgupta, Stephanie Cy Chan, Allison Tam, James Mcclelland, Chen Yan, Adam Santoro, Neil C Rabinowitz, Jane Wang, and Felix Hill. Tell me why! Explanations support learning relational and causal structure. In *Proceedings of the 39th International Conference on Machine Learning*, volume 162 of *Proceedings of Machine Learning Research*, pp. 11868–11890. PMLR, 2022.

Greg Landrum. Rdkit: Open-source cheminformatics, 2006. URL http://www.rdkit.org.

Robert Tjarko Lange, Yingtao Tian, and Yujin Tang. Large language model-based evolutionary optimizer: Reasoning with elitism. *arXiv preprint arXiv:2403.02054*, 2024.

Tiqing Liu, Yuhmei Lin, Xin Wen, Robert N Jorissen, and Michael K Gilson. Bindingdb: a web-accessible database of experimentally determined protein–ligand binding affinities. *Nucleic Acids Research*, 35(suppl_1):D198–D201, 2007. doi: 10.1093/nar/gkl999.

Shayne Longpre, Le Hou, Tu Vu, Albert Webson, Hyung Won Chung, Yi Tay, Denny Zhou, Quoc V. Le, Barret Zoph, Jason Wei, and Adam Roberts. The flan collection: Designing data and methods for effective instruction tuning. *ICML*, 2023.

Anton Lozhkov, Raymond Li, Loubna Ben Allal, Denis Kocetkov, Chenghao Mou, Christopher Akiki, Carlos Muñoz Ferrandis, Muennighoff Niklas, Jean Kaddour, Yacine Jernite, et al. Starcoder 2 and the stack v2: The next generation. *arXiv preprint arXiv:2402.19173*, 2024.

Aman Madaan, Niket Tandon, Prakhar Gupta, Skyler Hallinan, Luyu Gao, Sarah Wiegreffe, Uri Alon, Nouha Dziri, Shrimai Prabhumoye, Yiming Yang, Sean Welleck, Bodhisattwa Prasad Majumder, Shashank Gupta, Amir Yazdanbakhsh, and Peter Clark. Self-refine: Iterative refinement with self-feedback. *arXiv preprint arXiv:2303.17651*, 2023.

David Mendez, Anna Gaulton, A Patrícia Bento, Jon Chambers, Marleen De Veij, Eloy Félix, María Paula Magariños, José F Mosquera, Prudence Mutowo, Michał Nowotka, et al. Chembl: towards direct deposition of bioassay data. *Nucleic Acids Research*, 47(D1):D930–D940, 2019. doi: 10.1093/nar/gky1075.

Remi Munos, Michal Valko, Daniele Calandriello, Mohammad Gheshlaghi Azar, Mark Rowland, Zhaohan Daniel Guo, Yunhao Tang, Matthieu Geist, Thomas Mesnard, Côme Fiegel, Andrea Michi, Marco Selvi, Sertan Girgin, Nikola Momchev, Olivier Bachem, Daniel J Mankowitz, Doina Precup, and Bilal Piot. Nash learning from human feedback. In *Proceedings of the 41st International Conference on Machine Learning*, volume 235 of *Proceedings of Machine Learning Research*, pp. 36743–36768. PMLR, 2024.

Arkadi S Nemirovski and David Borisovich Yudin. *Problem Complexity and Method Efficiency in Optimization*. Wiley-Interscience, New York, 1983.

Yurii Nesterov and Vladimir Spokoiny. Random gradient-free minimization of convex functions. *Foundations of Computational Mathematics*, 17(2):527–566, 2017. doi: 10.1007/s10208-015-9296-2.

Allen Nie, Ching-An Cheng, Andrey Kolobov, and Adith Swaminathan. The importance of directional feedback for llm-based optimizers. *arXiv preprint arXiv:2405.16434*, 2024.

Erik Nijkamp, Bo Pang, Hiroaki Hayashi, Lifu Tu, Huan Wang, Yingbo Zhou, Silvio Savarese, and Caiming Xiong. Codegen: An open large language model for code with multi-turn program synthesis. *arXiv preprint arXiv:2203.13474*, 2022.

Marcus Olivecrona, Thomas Blaschke, Ola Engkvist, and Hongming Chen. Molecular de novo design through deep reinforcement learning. *Journal of Cheminformatics*, 9(1):1–14, 2017. doi: 10.1186/s13321-017-0235-x.

OpenAI. Openai o1 system card. Technical report, OpenAI, 2024. URL https://arxiv.org/abs/2412.16720.

Krista Opsahl-Ong, Michael J Ryan, Josh Purtell, David Broman, Christopher Potts, Matei Zaharia, and Omar Khattab. Optimizing instructions and demonstrations for multi-stage language model programs. *arXiv preprint arXiv:2406.11695*, 2024.

Long Ouyang, Jeffrey Wu, Xu Jiang, Diogo Almeida, Carroll Wainwright, Pamela Mishkin, Chong Zhang, Sandhini Agarwal, Katarina Slama, Alex Ray, John Schulman, Jacob Hilton, Fraser Kelton, Luke Miller, Maddie Simens, Amanda Askell, Peter Welinder, Paul F Christiano, Jan Leike, and Ryan Lowe. Training language models to follow instructions with human feedback. *Advances in Neural Information Processing Systems*, 35:27730–27744, 2022.

Aaron Parisi, Yao Zhao, and Noah Fiedel. Talm: Tool augmented language models. *arXiv preprint arXiv:2205.12255*, 2022.

Reid Pryzant, Dan Iter, Jerry Li, Yin Tat Lee, Chenguang Zhu, and Michael Zeng. Automatic prompt optimization with "gradient descent" and beam search. *arXiv preprint arXiv:2305.03495*, 2023.

Valentina Pyatkin, Saumya Malik, Victoria Graf, Hamish Ivison, Shengyi Huang, Pradeep Dasigi, Nathan Lambert, and Hannaneh Hajishirzi. Generalizing verifiable instruction following. *arXiv preprint arXiv:2507.02833*, 2025.

Yujia Qin, Shengding Hu, Yankai Lin, Weize Chen, Ning Ding, Ganqu Cui, Zheni Zeng, Yufei Huang, Chaojun Xiao, Chi Han, Yi Ren Fung, Yusheng Su, Huadong Wang, Cheng Qian, Runchu Tian, Kunlun Zhu, Shihao Liang, Xingyu Shen, Bokai Xu, Zhen Zhang, Yining Ye, Bowen Li, Ziwei Tang, Jing Yi, Yuzhang Zhu, Zhenning Dai, Lan Yan, Xin Cong, Yaxi Lu, Weilin Zhao, Yuxiang Huang, Junxi Yan, Xu Han, Xian Sun, Dahai Li, Jason Phang, Cheng Yang, Tongshuang Wu, Heng Ji, Zhiyuan Liu, and Maosong Sun. Tool learning with foundation models. *arXiv preprint arXiv:2304.08354*, 2023.

Rafael Rafailov, Archit Sharma, Eric Mitchell, Stefano Ermon, Christopher D Manning, and Chelsea Finn. Direct preference optimization: Your language model is secretly a reward model. *arXiv preprint arXiv:2305.18290*, 2023.

Baptiste Roziere, Jonas Gehring, Fabian Gloeckle, Sten Sootla, Itai Gat, Xiaoqing Ellen Tan, Yossi Adi, Jingyu Liu, Tal Remez, Jérémy Rapin, Artyom Kozhevnikov, Ivan Evtimov, Joanna Bitton, Manish Bhatt, Cristian Canton Ferrer, Aaron Grattafiori, Wenhan Xiong, Alexandre Défossez, Jade Copet, Faisal Azhar, Hugo Touvron, Louis Martin, Nicolas Usunier, Thomas Scialom, and Gabriel Synnaeve. Code llama: Open foundation models for code. *arXiv preprint arXiv:2308.12950*, 2023.

William Saunders, Catherine Yeh, Jeff Wu, Steven Bills, Long Ouyang, Jonathan Ward, and Jan Leike. Self-critiquing models for assisting human evaluators. *arXiv preprint arXiv:2206.05802*, 2022.

Jérémy Scheurer, Jon Ander Campos, Jun Shern Chan, Angelica Chen, Kyunghyun Cho, and Ethan Perez. Training language models with language feedback at scale. *arXiv preprint arXiv:2303.16755*, 2023.

Timo Schick, Jane Dwivedi-Yu, Roberto Dessì, Roberta Raileanu, Maria Lomeli, Luke Zettlemoyer, Nicola Cancedda, and Thomas Scialom. Peer: A collaborative language model. *arXiv preprint arXiv:2208.11663*, 2022.

Timo Schick, Jane Dwivedi-Yu, Roberto Dessì, Roberta Raileanu, Maria Lomeli, Luke Zettlemoyer, Nicola Cancedda, and Thomas Scialom. Toolformer: Language models can teach themselves to use tools. *NeurIPS*, 2023.

Zhihong Shao, Peiyi Wang, Qihao Zhu, Runxin Xu, Junxiao Song, Xiao Bi, Haowei Zhang, Mingchuan Zhang, YK Li, Yang Wu, et al. Deepseekmath: Pushing the limits of mathematical reasoning in open language models. *arXiv preprint arXiv:2402.03300*, 2024.

David Silver and Richard S. Sutton. Welcome to the era of experience. In *Designing an Intelligence*. MIT Press, 2025. Preprint.

Charlie Snell, Jaehoon Lee, Kelvin Xu, and Aviral Kumar. Scaling llm test-time compute optimally can be more effective than scaling model parameters. *arXiv preprint arXiv:2408.03314*, 2024.

Tianxiang Sun, Zhengfu Chen, Xipeng Qiu, and Xuanjing Huang. Bbtv2: Towards a gradient-free future with large language models. *arXiv preprint arXiv:2205.11200*, 2022.

The UniProt Consortium. Uniprot: the universal protein knowledgebase in 2023. *Nucleic Acids Research*, 51(D1):D523–D531, 2023. doi: 10.1093/nar/gkac1052.

Austin Tripp, Gregor N. C. Simm, and José Miguel Hernández-Lobato. A fresh look at de novo molecular design benchmarks. In *NeurIPS 2021 AI for Science Workshop*, 2021. URL https://openreview.net/forum?id=gS3XMun4cl_.

Jiayi Wang, Yuxuan Sun, Wenjia Zhang, et al. Adaptive preference scaling for reinforcement learning with human feedback. *arXiv preprint arXiv:2406.02764*, 2024.

Lei Wang, Chen Ma, Xueyang Feng, Zeyu Zhang, Hao Yang, Jingsen Zhang, Zhiyuan Chen, Jiakai Tang, Xu Chen, Yankai Lin, et al. A survey on large language model based autonomous agents. *arXiv preprint arXiv:2308.11432*, 2023a.

Yue Wang, Hung Le, Akhilesh Deepak Gotmare, Nghi D.Q. Bui, Junnan Li, and Steven C.H. Hoi. Codet5+: Open code large language models for code understanding and generation. *Proceedings of EMNLP*, 2023b.

Jason Wei, Maarten Bosma, Vincent Y. Zhao, Kelvin Guu, Adams Wei Yu, Brian Lester, Nan Du, Andrew M. Dai, and Quoc V. Le. Finetuned language models are zero-shot learners. *ICLR*, 2022a.

Jason Wei, Xuezhi Wang, Dale Schuurmans, Maarten Bosma, Brian Ichter, Fei Xia, Ed H. Chi, Quoc V. Le, and Denny Zhou. Chain-of-thought prompting elicits reasoning in large language models. In *NeurIPS*, 2022b.

David Weininger. Smiles, a chemical language and information system. 1. introduction to methodology and encoding rules. *Journal of Chemical Information and Computer Sciences*, 28(1):31–36, 1988. doi: 10.1021/ci00057a005.

Sean Welleck, Ximing Lu, Peter West, Faiz Karim, Liwei Jiang, Khyathi Chandu, Nouha Dziri, Ronan Le Bras, Lianhui Qin, Yu Gu, Rachel Rudinger, and Yejin Choi. Generating sequences by learning to self-correct. *ICLR*, 2023.

Christian Wirth, Riad Akrour, Gerhard Neumann, and Johannes Fürnkranz. A survey of preference-based reinforcement learning methods. *Journal of Machine Learning Research*, 18(136):1–46, 2017.

Wei Xiong, Hanze Dong, Chenlu Ye, Han Zhong, Nan Jiang, and Tong Zhang. Iterative preference learning from human feedback: Bridging theory and practice for rlhf under kl-constraint. *arXiv preprint arXiv:2312.11456*, 2023.

Chengrun Yang, Xuezhi Wang, Yifeng Lu, Hanxiao Liu, Quoc V. Le, Denny Zhou, and Xinyun Chen. Large language models as optimizers. *arXiv preprint arXiv:2309.03409*, 2023.

Shunyu Yao, Dian Yu, Jeffrey Zhao, Izhak Shafran, Thomas L. Griffiths, Yuan Cao, and Karthik Narasimhan. Tree of Thoughts: Deliberate problem solving with large language models. 2023a.

Shunyu Yao, Jeffrey Zhao, Dian Yu, Nan Du, Izhak Shafran, Karthik Narasimhan, and Yuan Cao. React: Synergizing reasoning and acting in language models. *ICLR*, 2023b.

Mert Yuksekgonul, Federico Bianchi, Joseph Boen, Sheng Liu, Pan Lu, Zhi Huang, Carlos Guestrin, and James Zou. Textgrad: Automatic "differentiation" via text. *arXiv preprint arXiv:2406.07496*, 2024.

Eric Zelikman, Yuhuai Wu, Jesse Mu, and Noah D. Goodman. Star: Bootstrapping reasoning with reasoning. *arXiv preprint arXiv:2203.14465*, 2022.

Shengyu Zhang, Linfeng Dong, Xiaoya Li, Sen Zhang, Xiaofei Sun, Shuhe Wang, Jiwei Li, Runyi Hu, Tianwei Zhang, Fei Wu, et al. Instruction tuning for large language models: A survey. *arXiv preprint arXiv:2308.10792*, 2024.

Xiang Zhou, Yuxuan Liu, Zhiyuan Chen, et al. Towards thinking-optimal scaling of test-time compute for llm reasoning. *arXiv preprint arXiv:2502.18080*, 2025.

Yongchao Zhou, Andrei Ioan Muresanu, Ziwen Han, Keiran Paster, Silviu Pitis, Harris Chan, and Jimmy Ba. Large language models are human-level prompt engineers. *arXiv preprint arXiv:2211.01910*, 2022.

Qihao Zhu, Daya Guo, Zhihong Shao, Dejian Yang, Peiyi Wang, Runxin Xu, Y Wu, Yukun Li, Huazuo Gao, Shirong Ma, et al. Deepseek-coder-v2: Breaking the barrier of closed-source models in code intelligence. *arXiv preprint arXiv:2406.11931*, 2024.

A Formal Statements and Proofs

Proposition 1 (Linear convergence under PL with rationale-guided directions). *Let $r : Z \to \mathbb{R}$ be L-smooth and satisfy the μ-PL condition (for maximization)*

$$\frac{1}{2}\|\nabla r(z)\|_2^2 \;\geq\; \mu\big(r(z^\star) - r(z)\big) \qquad \forall z \in Z.$$

At iteration t, suppose a direction v_t satisfies

$$\mathbb{E}[\, v_t \mid z_t \,] \;=\; \alpha\, \nabla r(z_t), \qquad \mathbb{E}\big[\, \|v_t - \mathbb{E}[v_t \mid z_t]\|_2^2 \,\big|\, z_t\big] \;\leq\; \sigma^2 \|\nabla r(z_t)\|_2^2,$$

with constants $\alpha > 0$ and $\sigma \geq 0$, and define $\kappa_1 \triangleq \alpha^2 + \sigma^2$. Consider the update $z_{t+1} = z_t + \eta v_t$. If a constraint set Z is present, assume $z_t + \eta v_t \in Z$ (i.e., the projection is inactive). With stepsize $\eta = \alpha/(L\kappa_1)$,

$$\mathbb{E}\big[r(z^\star) - r(z_{t+1}) \,\big|\, z_t\big] \;\leq\; \Big(1 - \tfrac{\mu\,\alpha^2}{L\,\kappa_1}\Big)\,\big[r(z^\star) - r(z_t)\big].$$

Unrolling yields

$$\mathbb{E}[r(z^\star) - r(z_T)] \;\leq\; \Big(1 - \tfrac{\mu\,\alpha^2}{L\,\kappa_1}\Big)^T\,\big[r(z^\star) - r(z_0)\big],$$

so ϵ-accuracy is achieved in

$$T \;=\; O\Big(\frac{L(\alpha^2+\sigma^2)}{\mu\,\alpha^2}\,\log\frac{1}{\epsilon}\Big)$$

iterations.

Proof. L-smoothness gives the two-sided bound

$$r(z_t + \eta v_t) \;\geq\; r(z_t) + \eta\langle \nabla r(z_t), v_t\rangle - \tfrac{L}{2}\eta^2\|v_t\|_2^2.$$

Taking conditional expectation and using $\mathbb{E}[v_t|z_t] = \alpha\nabla r(z_t)$ and $\mathbb{E}\big[\|v_t\|_2^2 \,\big|\, z_t\big] \leq (\alpha^2 + \sigma^2)\,\|\nabla r(z_t)\|_2^2 = \kappa_1\|\nabla r(z_t)\|_2^2$,

$$\mathbb{E}[r(z_{t+1}) \mid z_t] \;\geq\; r(z_t) + \Big(\eta\alpha - \tfrac{L}{2}\eta^2\kappa_1\Big)\,\|\nabla r(z_t)\|_2^2.$$

By the PL inequality, $\|\nabla r(z_t)\|_2^2 \geq 2\mu\,[r(z^\star) - r(z_t)]$, so

$$\mathbb{E}[r(z^\star) - r(z_{t+1}) \mid z_t] \;\leq\; \Big(1 - 2\mu\eta\alpha + \mu L\eta^2\kappa_1\Big)\,[r(z^\star) - r(z_t)].$$

Choosing $\eta = \alpha/(L\kappa_1)$ makes the bracket equal to $1 - \mu\alpha^2/(L\kappa_1)$, yielding the claim. □

A.1 Query Complexity and Dimension Dependence

Dimension-Free Case. When rationales provide full gradient information ($v_t \in \mathbb{R}^d$) at unit cost, the query complexity equals T and is dimension-independent:

$$\text{Queries} = O\left(\frac{L(\alpha^2+\sigma^2)}{\alpha^2\mu}\log\frac{1}{\epsilon}\right) \tag{3}$$

Coordinate-Sparse Case. Suppose each query reveals one coordinate of $\nabla r(z_t)$ chosen uniformly at random. Using the unbiased estimator $v_t = d\,(\partial_i r(z_t))\,e_i$ with $i \sim \mathrm{Unif}([d])$ gives $\alpha = 1$, $\sigma^2 = d - 1$, and hence $\kappa_1 = d$ and stepsize $\eta = 1/(Ld)$. We have

$$T = O\Big(\frac{Ld}{\mu}\log\frac{1}{\epsilon}\Big), \qquad \text{Queries} = O\Big(\frac{Ld}{\mu}\log\frac{1}{\epsilon}\Big).$$

Equivalently, averaging m independent coordinate queries per iteration yields $\sigma^2 = (d-1)/m$; taking $m = d$ recovers $T = O((L/\mu)\log(1/\epsilon))$ with d queries per iteration, so total queries remain $\Theta\big(\frac{Ld}{\mu}\log\frac{1}{\epsilon}\big)$.

This clarifies when and why dimension appears in the complexity.

B Lower Bounds for Exhaustive/Random Zeroth-Order Search

We formalize the intrinsic slowness of exhaustive (grid) search and best-of-N random sampling when only function values (or preferences) are used without directional information. The hard instance is the strongly concave quadratic

$$r(z) \;=\; r(z^\star) - \tfrac{\mu}{2}\,\|z - z^\star\|_2^2, \qquad z \in B_R(z^\star) \subset \mathbb{R}^d,$$

whose ϵ-optimal set is the ball $B_{\rho_\epsilon}(z^\star)$ with radius $\rho_\epsilon = \sqrt{2\epsilon/\mu}$.

Proposition 2 (Grid-search lower bound)**.** *Let $B_R(z^\star) \subset \mathbb{R}^d$ and a hypercubic grid of spacing h. Its covering radius is $\rho = \frac{\sqrt{d}\,h}{2}$. To guarantee that* for all *placements of $z^\star$ there exists a grid point in the ϵ-optimal ball $B_{\rho_\epsilon}(z^\star)$ with $\rho_\epsilon = \sqrt{2\epsilon/\mu}$, it suffices that $\rho \le \rho_\epsilon$ (i.e., $h \le 2\rho_\epsilon/\sqrt{d}$). Furthermore, any such grid restricted to $B_R(z^\star)$ must contain at least*

$$N \;\ge\; \left(\frac{R}{\rho}\right)^d \;=\; \left(\frac{R\sqrt{d}}{2\rho_\epsilon}\right)^d \;=\; \left(\frac{\mu R^2 d}{8\,\epsilon}\right)^{d/2}$$

points. Hence exhaustive grid search is exponential in d and polynomial in $1/\epsilon$ with exponent $d/2$ on this family.

Proof. Coverage of $B_R(z^\star)$ by N balls of radius ρ centered at grid points implies $NV_d\rho^d \ge V_d R^d$, hence $N \ge (R/\rho)^d$. With $\rho = \sqrt{d}\,h/2$ and $h \le 2\rho_\epsilon/\sqrt{d}$, we obtain $N \ge (R\sqrt{d}/(2\rho_\epsilon))^d$. Substitute $\rho_\epsilon = \sqrt{2\epsilon/\mu}$ to conclude. □

Proposition 3 (Best-of-N random sampling lower bound)**.** *Draw $X_1, \dots, X_N \overset{i.i.d.}{\sim} \mathrm{Unif}(B_R(z^\star))$ and let $\hat{z} = \arg\max_i r(X_i)$ for $r(z) = r(z^\star) - \frac{\mu}{2}\|z - z^\star\|_2^2$. Then with $a \triangleq 2/d$,*

$$\mathbb{E}[r(z^\star) - r(\hat{z})] = \frac{\mu R^2}{2}\, N\,\mathrm{B}(1{+}a, N) = \frac{\mu R^2}{2}\,\Gamma(1{+}a)\,\frac{\Gamma(N+1)}{\Gamma(N+1+a)}.$$

Moreover, for all $d \ge 1$ (so $a \in (0, 2]$),

$$\frac{\Gamma(N+1)}{\Gamma(N+1+a)} \;\ge\; (N+2)^{-a},$$

and thus

$$\mathbb{E}[r(z^\star) - r(\hat{z})] \;\ge\; \frac{\mu R^2}{2}\,\Gamma\Big(1 + \frac{2}{d}\Big)\,(N+2)^{-\frac{2}{d}} \;=\; \Omega\big(N^{-\frac{2}{d}}\big).$$

Proof. Let $R_i = \|X_i - z^\star\|_2$ and $R_{\min} = \min_i R_i$. The CDF of $R_{\min}$ is $F(r) = 1 - (1 - (r/R)^d)^N$ for $r \in [0, R]$. Differentiating, $f(r) = Ndr^{d-1}R^{-d}(1 - (r/R)^d)^{N-1}$. Then

$$\mathbb{E}[R_{\min}^2] = \int_0^R r^2 f(r)\,dr = NR^2 \int_0^1 t^{\frac{2}{d}}(1-t)^{N-1}dt = NR^2\,\mathrm{B}\big(1 + \tfrac{2}{d},\, N\big),$$

where $t = (r/R)^d$ and B is the Beta function. Using $\mathrm{B}(a, b) = \frac{\Gamma(a)\Gamma(b)}{\Gamma(a+b)}$ gives the exact expression. For the bound, we use the inequality $\Gamma(N+1)/\Gamma(N+1+a) \ge (N+2)^{-a}$ which holds for all $a \in (0, 2]$ and $N \ge 1$. □

C Extended Experiment Section

C.1 Implementation Details

SVG Code Optimization. We employ a tournament-style approach where `gpt-5-mini` generates SVG/TikZ code that gets rendered to PNG images for pairwise aesthetic comparisons by a separate instance of the same model acting as judge. The system maintains a "champion" design that only updates when both A-vs-B and B-vs-A orderings consistently agree on a winner, accumulating winning rationales into the generation prompt to guide aesthetic improvements across iterations. The judge provides natural language rationales explaining aesthetic preferences that inform subsequent generations.

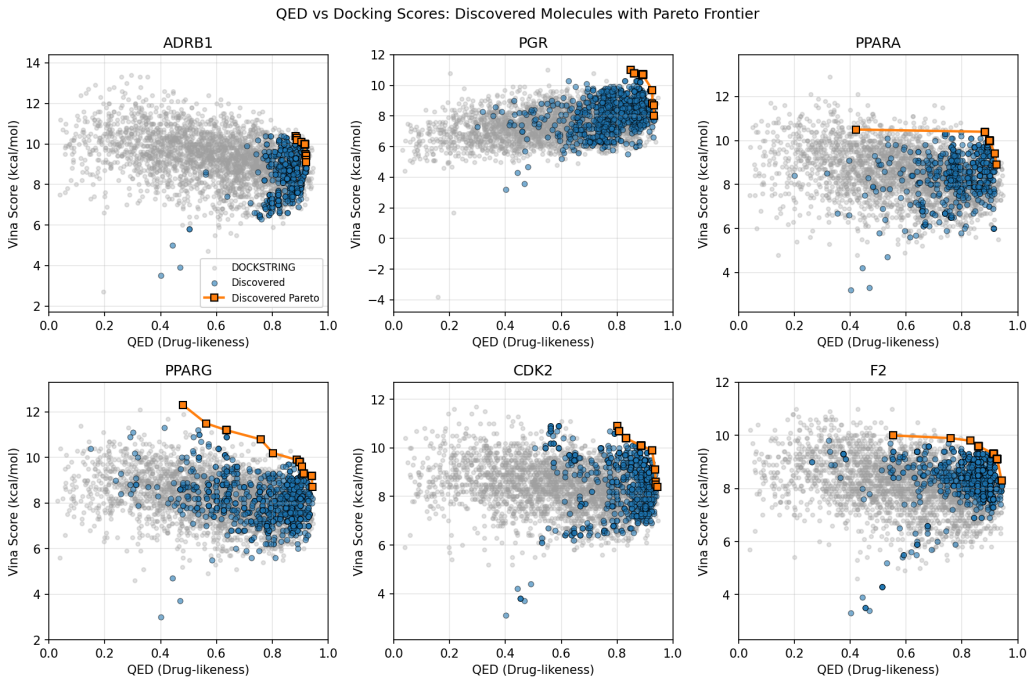

Figure 6: Pareto frontiers of discovered molecules (blue) compared against molecules in the DOCKSTRING dataset (gray) across six protein targets. The highlighted orange markers indicate molecules on the discovered Pareto frontier, achieving joint improvements in docking affinity (Vina score) and drug-likeness (QED).

IFBench Prompt Optimization. We closely follow the setting of Agrawal et al. (2025) for this experiment. We use their two-stage DSPy program with the `gpt-4.1-mini` model and temperature 1.0 for the solver and 0.0 for proposer/tagger to balance exploration and precision. To compare two prompts, we go through the training set to identify examples where program A succeeds and B fails, A fails and B succeeds, both fail, or both succeed, creating four explicit quadrants for analysis. We compute lift and precision/recall metrics on hypothesis tags, where lift measures the base rate of each event and the rate at which it occurs under a subset.

Molecule Optimization. We implement molecular optimization using the DOCKSTRING package (García-Ortegón et al., 2022) for protein-ligand docking simulations across six therapeutic targets. The system begins with three simple seed molecules (acetamide, pentane, benzene) and progressively evolves SMILES strings through iterative feedback loops that incorporate RDKit molecular properties, protein binding site information, and similarity comparisons to approved drugs as metadata. We use the combined score function suggested by DOCKSTRING:

$$s_{\text{overall}}(\text{molecule}, \text{protein}) = -\texttt{Vina}(\text{molecule}, \text{protein}) - 10 * (1 - \texttt{QED}(\text{molecule})), \quad (4)$$

where `Vina` provides the binding affinity prediction (kcal/mol, more negative is better) and the QED penalty term penalizes molecules with poor drug-likeness, with lower overall scores indicating better molecules that balance binding strength and drug-like properties. Note that QED scores range from 0 to 1 while Vina scores typically range from -3.0 to -12.0 kcal/mol. For Feedback Descent, we use a batch size of 8 and top-k selection of 10 examples.

C.2 Additional Results

Fig. 6 shows that across all protein targets, the discovered molecules extend beyond the DOCKSTRING baseline along both axes. The resulting Pareto frontiers illustrate consistent improvements in the joint trade-off between docking affinity and drug-likeness, highlighting that feedback-guided search yields coordinated gains rather than isolated outliers.

Fig. 7 shows optimization trajectories across all six protein targets. In each case, Feedback Descent reaches strong binding scores within the first few hundred oracle calls, while the competing specialized

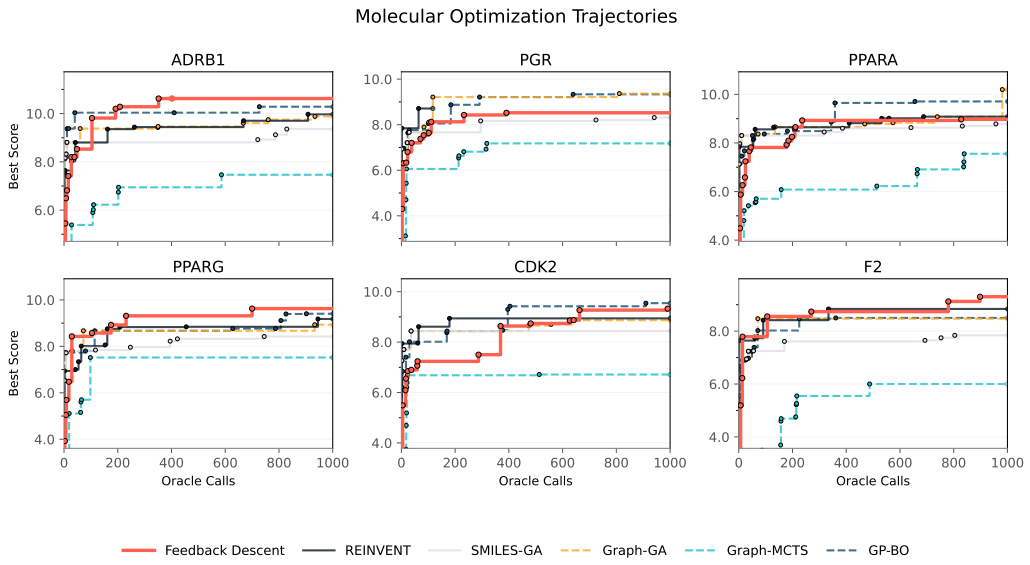

Figure 7: **Optimization trajectories across six protein targets.** Feedback Descent consistently attains higher docking scores with fewer oracle calls compared to standard molecular optimization baselines (REINVENT, SMILES-GA, GRAPH-GA, GRAPH-MCTS, GP-BO).

methods often plateau early (e.g., GRAPH-MCTS) or require substantially more evaluations to approach similar performance (e.g., SMILES-GA, GP-BO). Overall, the method is competitive with these baselines and in several cases outperforms them, suggesting that textual feedback provides a broadly effective and robust optimization signal across diverse binding targets.

C.3 Prompt Templates

We use the following prompt for the judge for the Anatomy SVG task. The rubrics for the other tasks are written in a similar style, translating a particular aesthetic into operational rules that minimize ambiguity.

Anatomy Judge Rubric

```
RUBRIC NAME: Anatomical Realism
INTENT: Believable equine anatomy with a plausible horn; form,
proportion, and structure matter most.

NON-NEGOTIABLES:
- Recognizable equine proportions; head, neck, torso, four legs, mane
, tail, horn present.
- Limbs connect anatomically; joints and hooves indicated.

CRITICAL BENCHMARKS (must evaluate these first):
1. Head-Neck Proportion: Neck length should be ~1.5 head length; head
 meets neck high on shoulders
2. Body Square: Body length (shoulder to buttock)  height at withers;
 chest depth  elbow height
3. Leg Structure: Proper joint articulation with elbow under withers;
 fetlock/pastern angles 45-55 when standing; all four limbs distinct
and correctly connected

WHAT TO REWARD:
- Correct limb count and articulation; mass distribution that could
stand or move.
```

```
- Horn integrates naturally with the skull (frontal bone center, 2-3"
 above eye line).
- Subtle shading or line variation conveying volume.
- Ground contact or cast shadow for grounding.
- Visible muscle definition suggesting tension/relaxation appropriate
 to pose.
- Differentiated hair textures: short coat vs coarse mane/tail
strands.
- Anatomical landmarks: withers prominence, gaskin curve.

WHAT TO PENALIZE:
- Missing or fused legs; impossible joints; balloon torsos.
- Flat cardboard profiles with no sense of volume.
- Decorative effects that obscure structure.
- Disney-fied proportions (oversized eyes, baby-like features).
- Horn placement anywhere except frontal bone center (2-3" above eye
line).

TIEBREAKERS:
- Prefer the image with more accurate limb/neck/head proportions.
- If both are plausible, choose the one with better weight and
grounding.
```

We use the following prompt templates for candidate generation and rationale generation for prompt optimization.

Prompt Template IFBench Candidate Generation

```
You are tasked with improving an assistant's prompt based on task
data, examples, and feedback.

## Current Prompts
**Approach A (Baseline):**
```python
{prompt_a_dict}
```

Approach B (Challenger):
```python
{prompt_b_dict}
```

Training Signals
{comparison}

Step 1: Task Inference
- Read the examples and feedback carefully.
- Infer the underlying task structure, required input/output forms,
and success criteria.
- Identify implicit constraints not explicitly stated in the original
 prompts.

Step 2: Knowledge Preservation
- Extract and encode domain-specific facts, constraints, and
conventions discovered in the examples.
- Include niche technical details that may not be obvious to a model
without this context.
- Distill general strategies the assistant used successfully.

Step 3: Failure Analysis
- Identify recurring mistakes and failure modes.
```

```
- Devise principle-based instructions to avoid them.
- When both approaches fail on a pattern, invent a new, generalizable
 strategy.

## Step 4: Prompt Synthesis
Write a new instruction prompt that:
1. Captures the task understanding (Step 1).
2. Preserves domain-specific facts (Step 2).
3. Embeds strategies that worked and guards against failures (Step 3)
.
4. Remains SHORT, PRINCIPLE-BASED, and free of training-set
overfitting.
5. Works robustly on UNSEEN TEST DATA.

The prompt must be a Python dictionary with the following keys:
{module_keys_description}

Output EXACTLY in this format:

```python
{prompt_template}
```"""
You are improving {artifact_type}. Here is the previous feedback:

Iteration 1: {rationale_1}
Iteration 2: {rationale_2}
...
Iteration {n}: {rationale_n}

Current best version:
{current_best}

Generate an improved version that addresses the feedback while
preserving existing strengths. Focus on the most actionable
suggestions from the rationales above.
```

Prompt Template for Molecule Optimization

```
You are a helpful assistant that proposes a single SMILES string
corresponding to a small molecule, based on the task explanation and
information about previous molecules that have been proposed. Your
proposed molecule should score highly on the {benchmark_name}
benchmark.

Task explanation: Maximize -{benchmark_name} - 10 * (1 - QED): larger
 values mean stronger {benchmark_name} binding and high drug-likeness
.
{protein_info_xml}

Your output format should be EXACTLY as follows:

<reasoning>[Chemical hypothesis linking structural changes to
expected binding/QED improvements]</reasoning>
<smiles>[Single SMILES string]</smiles>

Generate a small molecule based on these previous examples (sorted in
 descending order of score):

{examples_text}
```

Example of Protein Metadata (ADRB1)


```
{ 'target': 'ADRB1', 'accession': 'P08588', 'regions': { '
transmembrane': [[56, 84], [94, 120], [133, 154], [173, 196], [223,
248], [320, 349], [355, 377]], 'extracellular': [[1, 55], [121, 132],
 [197, 222], [350, 354]], 'cytoplasmic': [[85, 93], [155, 172], [249,
 319], [378, 477]], 'disordered': [[269, 307], [403, 477]]}, '
critical_residues': {'mutagenesis': [{'position': [474, 474], '
description': 'Loss of interaction with GOPC.'}, {'position': [474,
474], 'description': 'Loss of interaction with GOPC; when associated
with A-477.'}, {'position': [475, 475], 'description': 'Loss of
interaction with GOPC. Loss of interaction with RAPGEF2. Abolishes
agonist-induced Ras activation.'}, {'position': [475, 475], '
description': 'Loss of interaction with RAPGEF2.'}, {'position':
[475, 475], 'description': 'Partial loss of interaction with GOPC.'},
 {'position': [476, 476], 'description': 'Partial loss of interaction
 with GOPC.'}, {'position': [477, 477], 'description': 'Loss of
interaction with GOPC.'}, {'position': [477, 477], 'description': '
Loss of interaction with RAPGEF2. Abolishes agonist-induced Ras
activation.'}], 'natural_variants': [{'position': [26, 26], '
description': 'in dbSNP:rs34844626'}, {'position': [29, 29], '
description': 'in dbSNP:rs35720093'}, {'position': [31, 31], '
description': 'in dbSNP:rs35230616'}, {'position': [49, 49], '
description': 'correlated with low mean resting heart rate and
decreased mortality risk in patients with congestive heart failure;
dbSNP:rs1801252'}, {'position': [187, 187], 'description': 'found in
individuals with short sleep; results in decreased adenylate cyclase-
activating adrenergic receptor signaling; decreased protein stability
; dbSNP:rs776439595'}, {'position': [389, 389], 'description': '
increased beta1-adrenergic receptor activity; increased basal
activity and increased coupling to heterotrimeric G protein Gs that
stimulates the adenylyl cyclase; dbSNP:rs1801253'}, {'position':
[399, 399], 'description': 'in dbSNP:rs36052953'}, {'position': [405,
 405], 'description': 'in dbSNP:rs35705839'}]}}
```


Example of Molecule Metadata (CCCCC)


```
valid: 'True'
score: '-1.9121449019886678'
metadata:
  CanonicalSMILES: CCCCC
  InChIKey: OFBQJSOFQDEBGM-UHFFFAOYSA-N
  MolecularFormula: C5H12
  ExactMass: '72.093900384'
  FormalCharge: '0'
  AtomCount: '5'
  HeavyAtomCount: '5'
  HeteroAtomCount: '0'
  BondCount: '4'
  Sp3CarbonFraction: '1.0'
  RingCount: '0'
  AromaticRingCount: '0'
  AliphaticRingCount: '0'
  RotatableBondCount: '2'
  StereoCenterCount: '0'
  MurckoScaffold: ''
  LogP: '2.1965000000000003'
  TopologicalPolarSurfaceArea: '0.0'
  MolarRefractivity: '25.19899999999999'
  HBondDonorCount: '0'
  HBondAcceptorCount: '0'
```

```
  BertzComplexityIndex: '7.5097750043269365'
  BalabanJIndex: 2.19060968716425
  HallKierAlpha: '0.0'
  Kappa1: '5.0'
  Chi0v: '4.121320343559642'
  TotalEState: 8.5
  MinEState: 1.34375
  MaxEState: 2.2118055555555554
  PEOE_VSA6: '33.10993926815928'
  SlogP_VSA5: '33.10993926815928'
  BCUTp_1h: '13.744962415414642'
  AccessibleSurfaceArea: '34.19901948541599'
  FunctionalGroups: []
  StructuralAlerts: []
  QuantitativeDrugLikeness: '0.4687855098011332'
  SyntheticAccessibility: '1.699621281696647'
  NaturalProductLikeness: '0.09749981667944'
```

C.4 Discovered Prompts for IFBench

Below, we show the discovered prompts for Qwen3-8B and GPT-4.1-mini.

ensure_correct_response_module, Qwen3-8B (acc=44.22)

```
Extract every explicit constraint: order/sequence (e.g., repeat
verbatim first, nothing before it; required exact ending), verbatim
text/keywords (case, spacing, punctuation), forbidden items, numeric/
format limits (exact/min sentences, words, characters; counts of
letters/words/capitalized words; number/format of bullets/items),
tone/style, math/logic (units, rounding), and formatting bans (e.g.,
no code blocks). Build a checklist. Validate the draft: (1) If repeat
-first or 'nothing before' is required, ensure the very first
character starts the repeated text; copy it exactly; no quotes/
headers/spaces/blank lines before it. (2) If an exact ending is
required, the final characters are exactly that phrase with nothing
after. (3) All required phrases/keywords included as specified (
respect case/order if stated). (4) Numeric/format limits match
precisely, including sentence count and capitalized-word count;
control with short, simple sentences and standard punctuation; avoid
abbreviations/ellipses/decimals that can alter sentence counts unless
 necessary. (5) Math is correct; apply requested rounding/units. (6)
Tone met; no forbidden items. If constraints conflict, prioritize:
order/sequence > verbatim/ending > forbidden items > numeric/format
limits (incl. sentence and capitalized-word counts) > keywords/tone >
 any extras. Fix issues and re-check. Remove trailing spaces/newlines
.",
```

generate_response_module, Qwen3-8B (acc=44.22)

```
Read the prompt and list constraints: sequence (repeat verbatim first
; nothing before; required exact ending), scope of counts (entire
response vs answer only), exact phrases/keywords (case/order),
forbidden items, numeric limits (exact/min sentences, words,
characters; occurrences; number/format of bullets/items; count of
capitalized words), tone, and any math/logic with units/rounding.
Plan the structure accordingly. If required to repeat the request
verbatim at the beginning, copy it exactly and place it first with
nothing before; do not add quotes; then proceed to the answer (use a
single newline as a separator only if not forbidden). Scope all
```

```
counts as specified; if unspecified, apply them to the entire
response. Meet numeric limits exactly: control sentence count with
simple sentences and standard punctuation; avoid abbreviations/
ellipses/parentheticals; deliberately include the needed number of
Capitalized words and count them. Include required keywords/phrases
in the stated order/case; exclude forbidden items. Do computations
accurately; follow rounding/units. If a specific ending is required,
ensure your final characters are exactly that phrase. Provide step-by
-step explanation only if explicitly requested; otherwise be concise.
 Before finalizing, recount/recheck against the constraint list and
adjust. Remove trailing whitespace.
```

generate_response_module, GPT-4.1-mini (acc=54.59)

```
Pre-check for compliance and correctness: 1) Parse the task into a
compact internal spec: goal and success criteria; exact required
outputs; structure (counts/order/labels/delimiters); required first/
last tokens; exact literals to reproduce and their placement (
preserve casing/spacing/punctuation); content rules (required/
forbidden items and exact occurrence/length limits); language/
modality; numeric rules (use only provided data; units/conversions;
round only at the end); safety/policy limits. 2) Apply instruction
hierarchy (system > developer > user); resolve by specificity and
recency. If full compliance is impossible or unsafe, produce the
smallest safe compliant output; do not invent facts. 3) Numbers:
extract data and units, normalize units, compute precisely, verify
totals/consistency, delay rounding. 4) Verbatim/echo: copy literals
exactly, respect stated inclusion/exclusion boundaries, no
normalization or padding before/after echoed segments. 5) Final audit
: confirm structure and counts, required positions and boundary
tokens, verbatim exactness, occurrence/length limits, absence of
forbidden items, language/modality lock, numeric units and rounding,
safety compliance, and no extra text.
```

ensure_correct_response_module, GPT-4.1-mini (acc=54.59)

```
Plan then write: decide the exact output shape from the spec (
sections/items/order/labels/delimiters) and fix boundary tokens and
literal placements. Lock the requested language and modality. Use
only provided data for any calculations; normalize units; apply
rounding at the end. Draft the smallest content that satisfies all
constraints; enforce required/forbidden items and exact occurrence/
length counts while writing. Self-check and repair: recount structure
 and counts; verify first/last tokens and required positions; ensure
verbatim correctness with no added/omitted characters or padding;
confirm numeric correctness and units; ensure safety/policy
compliance. Output only the final compliant answer.
```